Kinetic-Isothermal modeling and statistical analysis of optimized parameters in batch adsorption study

Srinivas Tadepalli[1*], K.S.R. Murthy[2], H. Upender[3], Deepak Yadav[4,5*]

[1*]Department of Chemical Engineering, Imam Muhammad bin Saud Islamic University, Riyadh-11432, Saudi Arabia

[2] Department of Chemistry, College of Engineering studies, University of Petroleum and Energy Studies, Dehradun 248007, India

[3] Department of Chemical Engineering, National Institute of Technology Warangal, Warangal 506004, India.

[4]Chemical Engineering Department, Harcourt Butler Technical University (Formerly HBTI), Kanpur-208002, India

[5*] Department of Chemical Engineering, Meerut Institute of Engineering & Technology, Meerut - 250005, India

Abstract

The present work explores the kinetics, isothermal and statistical studies for the adsorption of Cu and Cd ions by adsorbent prepared by mixing activated charcoal, bone charcoal in 1:1 ratio in batch adsorption study. The batch experiments were performed for 2 hours in view of 6 parameters optimizing each of them. The data attained for the optimized parameters were studied concluded by fitting them for kinetic models pseudo-first and Pseudo-second order models along with regression coefficient (R^2) values. The statistical analysis of the data acquired in kinetic modeling delineated the control of pseudo-second order for both Cu and Cd adsorption with insignificant χ^2values**.** When the values were matched with pseudo-first order and Langmuir model intending dominancy for chemisorption. In this simultaneous metal ion removal process, the higher R^2 values were recognized with Cu (II) which envisages the restored suitability of the Langmuir model matched with Cd. The higher correlation coefficient (R^2) values for both Cu (II) and Cd (II) predict the suitability of Temkin isotherm model at the given adsorbent conditions.

Key words: Batch Study, Activated Charcoal, Bone Charcoal, Kinetics Model, Isotherm Model, Statistical Studies.

1. Introduction

Our Earth surface comprises of 70% water is the utmost valued natural source. Deprived this valuable compound, the life on the Earth would not exist. Even this fact is extensively accepted, while water pollution is a public problem being encountered nowadays. Heavy metal pollution arises straight by effluent drain out of refineries, industries, waste treatment plants and ultimately by the soils/ground water contaminants that enter the water supply from the atmosphere via rain water. Modern industrial effluent is mainly responsible for

contamination to the water bodies. Lakes, ponds, rivers and oceans are stunned with numerous toxic chemicals. Amongst toxic elements takeover hazardous levels are heavy metals. Commonly, heavy metals can be found in wastewater from industries. Heavy metals are one of the major classes of pollutants in industrial effluent. Among them are Cd (II), Pb (II), Fe (III), Cu (II), Mn (II), Ni (II), and Zn (II). Absorption of wastewater (containing heavy metal) by marine animals and indirectly move in the human food, existing a high risk to consumer. Heavy metals can also contaminate and accumulate in the soil for a long-term and it is seized in the soil on account of chemical reaction, adsorption and ion exchange of soil. Even though certain heavy metals are essential for the growth of plants, but above certain concentration level, the heavy metals turn into lethal for both plant and organisms. There are a lot of toxic heavy metals in chemical manufacturing, mining, tannery, battery manufacturing, metallurgical, etc. [1]. All of these will generate wastewater contaminated with hazardous heavy metals.

Metals are broadly used in few industries, with mining, electroplating, metallurgical, metal finishing and electronic. The presence of heavy metals in industrial effluent is particularly objectionable, by means of toxic nature. Under these environments, metals may accumulate to toxic levels and cause environmental damage.

Now a days, the main concern is the release of pollutants to the water bodies and which will cause adverse effect on living species. Copper and Iron are the most important and commonly used material which is associated with day to day life of human being. The major source of copper and Iron are the metal plating industries, which may release the coated water to environment without proper treatment and hence causing the potential hazards like lung cancer[1]. It is well known that there are various methods to reduce the concentration of these metal ions in the water bodies like precipitation, ion exchange, extraction operations, dialysis and electro dialysis etc [2–4] But all the above methods are not feasible in terms of economy for small and medium scale industries. But these techniques are lavish and inefficient when the concentration of metals are low (below 100ppm) and there is generation of large quantities of wastes. Development of eco-friendly, efficient and low - cost processes is the need of the hour and in this aspect, adsorption is a versatile technology with the advantages of high efficiency and selectivity for adsorbing metals in low concentrations, recycling of the adsorbent and minimization of the sludge generation. Hence, the adsorption operation is the preferred, broadly recycled technique for the heavy metal adsorption despite its low cost and ease of regeneration.

Adsorption denotes to the separation of solute particles in a confined space from a liquid phase (fluid phase) on to solid surface. The particle of the adsorbate comes from the fluid segment into the boundary, the place they persist for an interval of phase. In a rescindable method, the particles return to the segment from which they got here or reversibly cross into an alternative segment even as other particles exchange them at the boundary. On accomplishment of the solid surface, the adsorbed particles interchange energy with structural atoms of the outside surface and if enough period was once there for adsorption, the adsorbed particles and the surface atoms reach thermal stability. The quantity of molecules entering on the boundary in an assumed period is equivalent to the number of molecules parting the boundary to go into the fluid segment [5, 6]

Animal charcoal also known as bone black, bone char or abaiser, is a coarse material formed by charring animal bones. Animal bones are part of the composite that form the body of animals; it basically gives shape and support to animals (Skeletal systems). It contains about 12 % carbon, the remainder being calcium and magnesium (84 %) and other inorganic materials present in the bones [7]. Animal charcoal possesses a higher degree of removing coloring matters from solutions; charcoal is used in art of drawing in form of fine, compressed and powdered charcoal [8].

Activated carbon being a carbon form that has been treated to make it enormously porous and consequently have a large surface area offered for absorption or chemical reaction. Almost any carbonaceous material of animal, vegetable or mineral origin can be made into activated carbon when properly treated e.g. from animal bones, wood, corn cobs, coffee, beans, rice husks, fruit peels and nuts shells and minerals such as peat, soft and hard coal tar, asphalt, phloem residues and carbon black [9] Though there are many commercially available activated carbons, these are still quite expensive [10].Various researchers have carried out studies for simplified and cost-effective methods of activation carbon [11–13]. The most widely used activation carbon process are the treatment of the carbonaceous materials with oxidizing gases such as air, steam or carbon dioxide and the carbonization of the raw material's co-existence with chemical reagents such as zinc chloride, magnesium chloride, calcium chloride or phosphoric acid [14–17].The surface area per gram of an adsorbent is called the specific surface area [18]. The primary use of activated carbon is in removing pollutants from air or water stream both in the field and in industrial process such as spill cleanup, ground water remediation, portable water filtration, waste water treatment etc. Among the literarily hundreds of other uses are agents in gas masks, pollution control devices such as car catalytic converters and flue gas desulfurization[19]. Activated carbon is also used to remove pesticide residues [20]. Modified activated carbon derivative seeds of widely available plant source of *Martyniaannua L and Xanthiyamstrumarium*to study the physico-chemical properties of the agricultural waste[21].

2. Materials and Methodology

The following procedure describe about the chemicals used, adsorption preparation, detailed batch study procedure, analysis of Kinetic, Statistical, Isothermal modeling studies have been described in this paper.

2.1 Chemicals used

Analytical grade salts of $CuSO_4.H_2O$, $CdCl_2.H_2O$, purchased from Sigma Aldrich were used for the preparation of synthetic effluents. Activated charcoal (AC) and Bone charcoal (BC) procured from Sigma Aldrich (95% purity) were used as a mixed adsorbent by blending in (1:1 ratio) for this study.

2.2 Mixed adsorbent preparation

The mixed adsorbent was prepared by mixing activated charcoal (AC) and bone charcoal (BC), in 1:1 ratio and particle size analysis (Malvern, Malvern Instruments Ltd, United Kingdom) was carried out in particle size Analyzer to determine the particle size of the mixed adsorbent. The average particle size of the mixed adsorbent was reported as 572.2 nm.

2.3 Batch studies

Following a systematic procedure for the removal of heavy metal ions, initially the presterilizing flasks containing heavy metal ion solution of 50 mg/l of Cu (II) and Cd (II) were prepared and the mixed adsorbent of 0.5 g/L of mixed adsorbent was added after maintaining the desired pH. Adjustment of pH was done by adding 0.1 M NaOH / 0.1 M HCl. Adsorption process was carried out in the rotary shaker/agitator until the equilibrium was attained. The analysis was done for the filtered samples by Atomic Absorption Spectrophotometer (AAS) (Thermo Scientific) to find the residual concentrations at various time intervals from the collected samples. After the analysis equilibrium time and the residual concentration were reported. The statistics attained in the present readings were used to calculate the % removal of the heavy metal ions by

expending **Eq 1.** given below. Trials were done thrice and the average values were conveyed for the adsorption system.

The % removal was evaluated using the mathematical relationship given by

$$\textbf{\% removal} = \frac{C_o - C_e}{C_o} \textbf{ x 100} \qquad \textbf{(1)}$$

Where C_o, C_e is the initial, equilibrium concentration of metal ions in mg/l.

2.4 Characterization of the adsorbent

Physical characterization such as proximate and ultimate analysis[22].FTIR and BET analysis were carried out to determine the physico-chemical properties and different functional groups that were available for adsorption. The surface area of the mixed adsorbent and maize cob were found to be 951 and 636.6 m^2/g respectively [22].

2.4.1 BET analysis

BET theory explains the physical adsorption of N_2 gas on a solid surface, assists as basis for the specific surface area measurement of the mixed adsorbent [23]. The specific surface area of a powder (adsorbent) is regulated by physical adsorption of a gas on the adsorbent surface and the amount of adsorbate gas calculated corresponding to a monomolecular surface adsorption. Physical adsorption results after relatively weak forces (van der Waals forces) among the adsorbate (gas) molecules and the adsorbent (powder) surface area. The determination of specific surface area is frequently carried out at -196 °C. The quantity of gas adsorbed can be measured by a volumetric/ continuous flow process. The specific surface area of powder is assessed from the volume of nitrogen adsorbed versus pressure, at the boiling point temperature (BPT) of liquid nitrogen at normal atmospheric pressure (Make Micrometrics Gemini 2375)-Micro metrics Instrument Corporation, U.S.A.

The BET method indicates to a surface area constraint which allows to relate, categorize and evaluate different models and to consider pores (micro, meso and macro pores), roughness and particle shapes by dimensions[24]

The BET surface area which predicts from complete adsorption and desorption isotherms can be utilized as an integral parameter for the determination of pore volume and pore size supply. The BET surface area of the mixed adsorbent was found to be 951 m^2/g.

2.4.2 XRD Analysis

X-Ray Diffraction Analysis (XRD) examines crystalline structure, comprising atomic arrangement and imperfections. XRD analysis was established on constructive in- deference of monochromatic X-rays and a crystalline sample. The X-rays were produced by a cathode-ray tube, filtered to yield monochromatic radiations, collimated to focus towards the taster. The interface of the incident rays with the taster yields constructive interference and a diffracted ray once conditions fulfil Bragg's law. This law transmits the electromagnetic radiation wavelength to a diffraction angle and lattice spacing in the crystalline sample.

2.4.3 Proximate and Ultimate analysis

Proximate analysis is a type of assay for the determination of different constituents present in the coal sample. Standard procedures were followed to determine the bulk density, average particle size diameter, fixed carbon, volatile content, moisture content, ash content, and surface area. Ultimate analysis contributes the

composition of the sample in terms of wt% of carbon, nitrogen, hydrogen, oxygen and sulfur. The carbon content determination includes the carbon existing in the organic coal substance and as mineral carbonates. Hydrogen determination gives the hydrogen content in the organic materials with the coal. All the nitrogen resolute was expected to be the part of the organic materials in the coal. The results of the proximate and ultimate analysis, physical properties are reported here as shown below in table 1, table 2 and table 3 respectively.

Table 1: Proximate analysis of the mixed adsorbent

Property	Composition of the mixed Adsorbent
Bulk Density (g/cc)	0.74
Average particle diameter	572.2 nm
Moisture content	4.24%
Volatile matter	23.61%
Ash Content	4.39%
Fixed carbon	68.57%
Surface area (m^2/g)	951

Table 2 Ultimate Analysis of the mixed adsorbent

Component	Composition (%)
Carbon	65.12
Nitrogen	9.41
Hydrogen	6.63
Oxygen	18.85
High heating value	33.28

Table 3: Physical properties of the mixed adsorbent

Adsorbent type	Surface area (m^2/g)	Moisture (%)	Particle size (nm)	Charge
Pristine AC	1600	5	980	neutral
Pristine BC	267	3.43	681	-ve
50 % each	951	4.24	572.2	-ve

2.4.4 FTIR Analysis

An infrared spectrum represents a fingerprint of a sample with absorption peaks which correspond to the frequencies of vibrations between the bonds of the atoms making up the material. Because each different material is a unique combination of atoms, no two compounds produce the exact same infrared spectrum. Therefore, infrared spectroscopy can result in a positive identification (qualitative analysis) of every different kind of material. In addition, the size of the peaks in the spectrum is a direct indication of the amount of

material present.

Fourier Transform Infrared (FTIR) Spectroscopy is a technique used to determine qualitative and quantitative features of IR-active molecules in organic or inorganic solid, liquid or gas samples. It is a rapid and relatively inexpensive method for the analysis of solids that are crystalline, microcrystalline, amorphous, or films. Another advantage of the IR technique is that it also can provide information about the light elements such as hydrogen and carbon in inorganic substances. FTIR analysis has been carried out for the mixed adsorbent before and after adsorption of copper and cadmium and the results are reported in section 4.

2.4.5 Pore size distribution

The pore size distribution analysis of the mixed adsorbents has been carried out before and after adsorption for both copper and cadmium using liquid nitrogen gas at a temperature of -196°C using surface area analyzer and the total pore volumes of pores less than 314.768 nm was reported. Adsorption and desorption cumulative volumes of the pore between 1.7 and 300 nm, average pore width, adsorption, desorption average pore width before and after adsorption of copper and cadmium were reported here. After adsorption as the pores were blocked by the metal ions, both the pore volume and pore width has been decreased.

2.4.5.1 Pore size distribution of mixed adsorbent after adsorption

The pore size distribution of the mixed adsorption were shown after adsorption and the total pore volume of pores less than 243.28 nm diameter was reported for Cu (II) and Cd (II) as 0.3937 cm^3/g and 0.324 cm^3/g as revealed in the Figs. 1, 2 and 3 respectively. Adsorption and desorption increasing volumes of pores among 1.7000 nm and 300.0000 nm diameter were originate to be 0.2848 cm^3/g and 0.2987 cm^3/g respectively. The average pore width (4V/A by BET) was found to be 3.68 nm. Adsorption and desorption average pore width was found to be 5.01 nm and 4.51 nm respectively. After adsorption as the pores were blocked by the metal ions both the pore volume and the pore width has been decreased respectively.

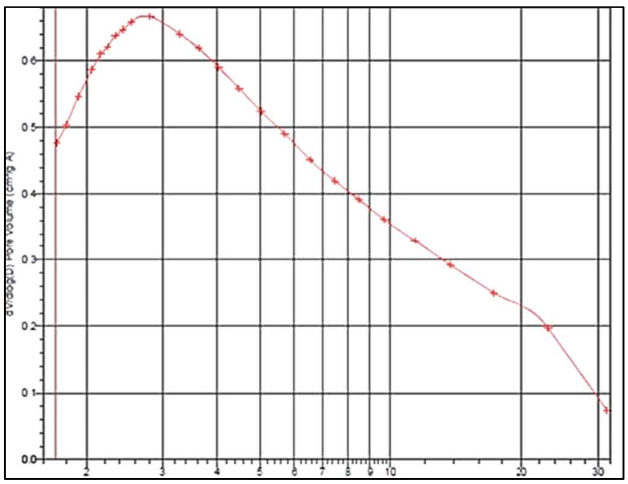

Figure 1: Pore size distribution of mixed adsorbent before adsorption

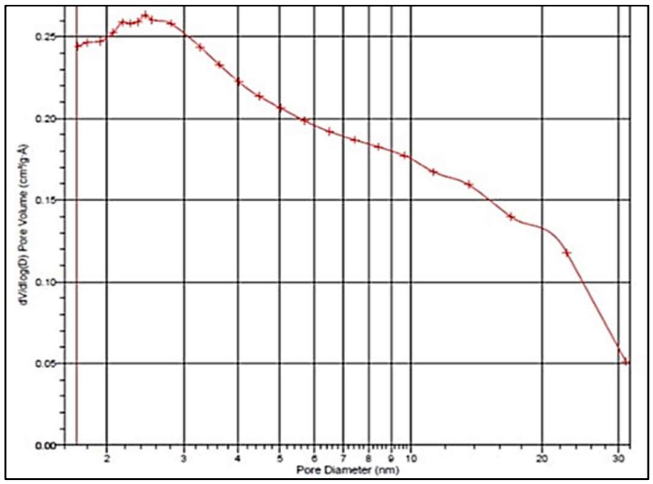

Figure 2: Pore size distribution of mixed adsorbent after adsorption of Cu (II)

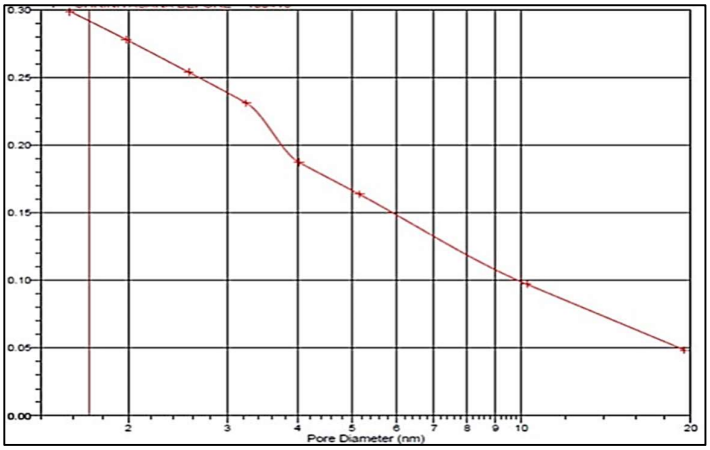

Figure 3: Pore size distribution of mixed adsorbent after adsorption of Cd (II)

2.4.6 Working of particle size analyzer

The particle size analyzer works on the principle of dynamic light scattering where He-Ne laser acts as a light source. There should be Brownian motion in the solution for the uniform distribution of the particle size. The Zetasizer Nano series performs size measurements using a process called dynamic light scattering (DLS). Dynamic Light Scattering (also known as PCS- Photon Correlation Spectroscopy) measures Brownian motion and relates this to the size of the particles. It does this by illuminating the particles with a laser and analyzing the intensity fluctuations in the scattered light. The results of the particle size of the mixed adsorbent is shown in figure 4.

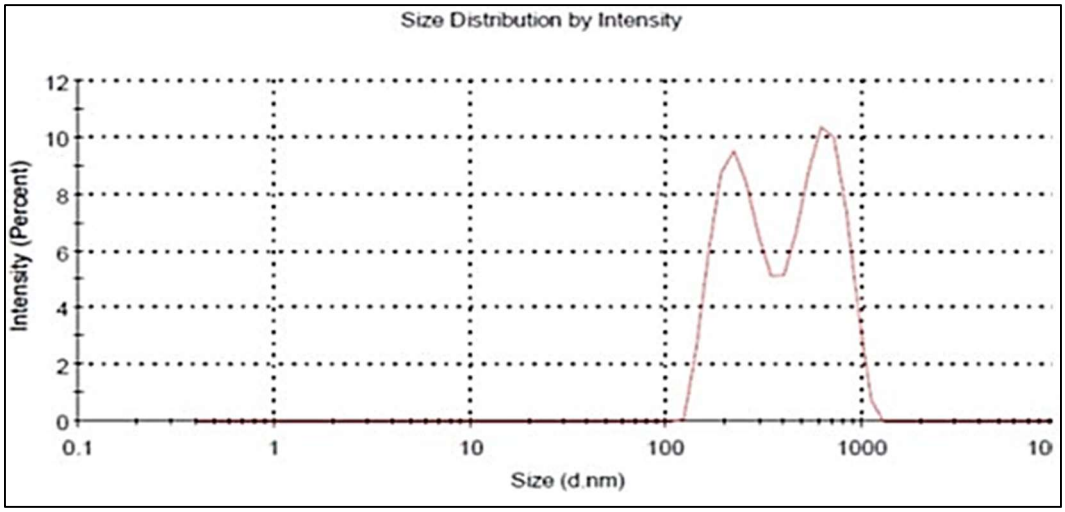

Figure 4: Particle size of the mixed adsorbent

3. Results and discussion

The kinetic models include the pseudo-first order and pseudo-second order equations. The pseudo-first order and second order modeling studies has been carried out for both the metals copper and cadmium at the optimized conditions obtained for each parameter in the batch study (pH 6, T = 40 °C, initial metal ion concentration of 100 ppm and adsorbent dosage of 5 g/L). Table 4 shows the optimized parameters of the batch adsorption study.

Table 4 Optimized parameters of the batch adsorption study

Parameters	Optimized value
pH	6
MIC (ppm)	100
Temperature(°C)	40
Adsorbent dose (g/L)	5

3.1 Model equation for batch studies

With the intention of research, the system of adsorption and the potential rate controlling step; for example, chemical reaction and transport phenomena, dynamic models were utilized to test the obtained data. The kinetic models include the pseudo-first order and pseudo-second order model.[25]

3.1.1 Pseudo-first order equation

In view of the desorption of metal ions with adsorption on active sites present on adsorbent surface, the rate of adsorption is directly proportional to the number of vacant sites [24, 25].The pseudo-first order equation was represented by [25] **Eq. 2:**

$$\frac{dq}{dt} = k_1 (q_e - q_t) \qquad (2)$$

where q_e and q_t are the adsorption capacity at equilibrium, and at time t respectively (mg/g). k_1 is the rate constant of pseudo-first order equation (min^{-1}). Integrating the above equation and applying the boundary conditions (t = 0 to t = t, and q_t = 0 to $q_t = q_t$), the integrated form of Eq.**2** turn out to be [25]

$$\log (q_e - q_t) = \log (q_e) - \frac{k_1 t}{2.303} \quad (3)$$

Eq. 2 is valid to the experiment outcomes but usually varies from a true first order equation in two ways: (i) The parameter $k_1(q_e-q_t)$ does not signify the number of accessible sites and (ii) the constraint $\log(q_e)$ is a variable parameter and frequently it was originate not equal to the intercept of a plot between $\log (q_e-q_t)$ vs t, where as in an accurate first order $\log(q_e)$ should fit for the intercept of the plot drawn between $\log (q_e-q_t)$ versus t.[25]

With the aim of fitting the equation to the experimental data [25] the equilibrium adsorption capacity q_e must be identified. In many cases q_e is unidentified and as chemisorption inclined to convert immeasurably slow[7], the volume adsorbed is quiet expressively reduced to the equilibrium uptake capacity . In most of the cases in the literature, pseudo-first-order equation of Lagergren does not fit well for the entire series of contact time and is mostly valid over the initial period of 20 to 30 minutes after the start of adsorption process.[7] [26]

A plot of $\log (q_e-q_t)$ against time was plotted for the obtained data at the elevated parameters for pH = 6, T = 40°C, initial metal ion concentration of 100 ppm, adsorbent dosage of 5g/L for both the metal ions to find the correlation coefficient or coefficient of Regression (R^2) which holds a straight-line relationship and the parameters q_e and $k_1$can be determined from the intercept and slope respectively. The slope and intercept values were shown in **Tables 5 and 6** for both the metals (Cu and Cd respectively) at the optimized conditions.

It can be concluded that the coefficient of regression (R^2) values are close to 1 in case of Cu (II) at adsorbent dosage of 5 g/L and temperature of 40°C which indicates that the adsorption systems follow the Pseudo first order equation for copper as compared to cadmium shown in **Tables 5 and 6** respectively. The table gives the data about the first order rate constant k_1 in min^{-1} and q_e in mg/g which was obtained theoretically from the slope and intercept

respectively from **Figs. 5 to 8**. It can be concluded that the data fits well for Cu (II) than Cd (II) with higher R^2 values in case of copper [27]

Table 5 Pseudo-first order model equation for Cu (II) at optimized conditions

PFOE conditions	Model equation	k_1 (min^{-1})	R^2	q_e (mg/g)
pH 6	y= -0.0146x+0.078	0.0336	0.8192	1.2
T = 40°C	y= -0.0147x+0.51	0.0338	0.886	3.23
MIC = 100 ppm	y = 0.0113x-0.19	0.026	0.6064	0.646
Adsorbent dosage 5 g/L	y=-0.0138x-1.21	0.0318	0.97	0.06

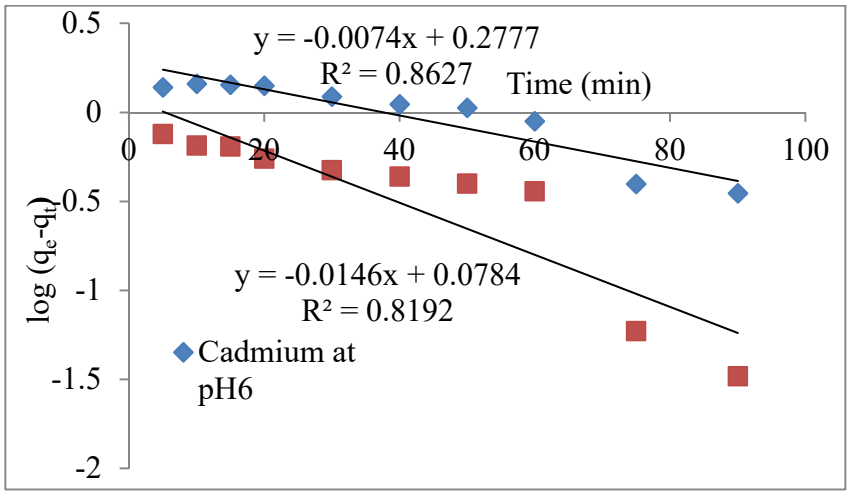

Fig 5 Pseudo first order equation for copper and cadmium at pH 6

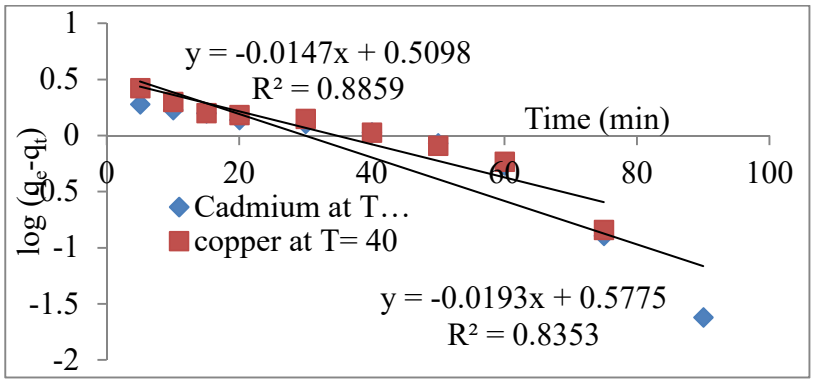

Fig 6 Pseudo first order equation for copper and cadmium at T = 40°C

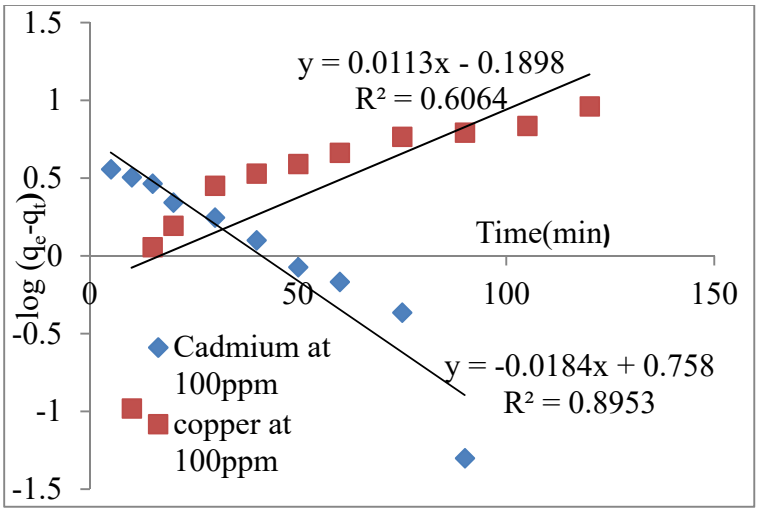

Fig 7 Pseudo first order equation for copper and cadmium at MIC of 100 ppm

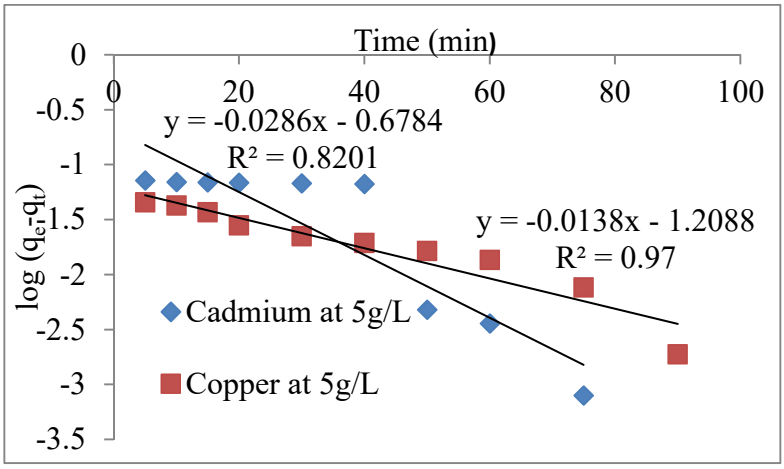

Fig 8 Pseudo first order equation for copper and cadmium at 5 g/L of adsorbent dosage

Table 6 Pseudo first order equation for Cd (II) at optimized conditions

PFOE conditions	Model equation	k (min^{-1})	R^2	q_e (mg/g)
pH 6	y= -0.0074x+0.0278	0.017	0.863	1.9
T = 40 °C	y = -0.019 x+ 0.578	0.044	0.835	3.8
MIC = 100 ppm	y = -0.0184x+0.76	0.042	0.895	5.73
Adsorbent dosage 5 g/L	y= - 0.0286x-0.679	0.066	0.82	0.21

3.1.2 Pseudo-second order equation

Here in this model it was anticipated that adsorption, binding of metal ion or adsorbate on the adsorbent surface is facilitated by chemical forces instead of physical forces of attraction [28]

Non-linear form of the model is given as

$$\frac{dq}{dt} = k_2(q_e - q_t)^2 \quad \textbf{(4)}$$

Upon integration with boundary conditions from $q_t = 0$ at $t = 0$, $q = q_t$ at $t = t$, the above **Eq.4** reduces to

$$\frac{t}{q_t} = \frac{1}{k_2 q_e^2} + \frac{t}{q_e} \quad \textbf{(5)}$$

where, q_e and q_t are the adsorption capacities at equilibrium, and at time t, correspondingly (mg/g). k_2 is the rate constant of pseudo-second order equation (g/mg.min). A plot of t/q_t vs t for the pseudo-second order equation holds a straight-line correlation and the parameters q_e and k_2 can be resolute from slope and the intercept. A graph of t/q_t vs t at diverse optimized conditions of pH 6, T = 40°C and initial metal ion concentration of 100 ppm, 5g/L of adsorbent dosage for both the metal ions was plotted to find the correlation coefficient or coefficient of regression (R^2) that determines the best fit equation and the parameters q_e and k_2 can be calculated from the slope and intercept. It can be concluded that the coefficient of regression (R^2) values are adjacent to 1 in Cu (II) and Cd (II) at adsorbent dosage of 5g/L, temperature of 40°C, pH 6 and initial metal ion concentration (C_o) of 100 ppm which indicates that the adsorption system monitors the pseudo-second order equation for both copper and cadmium as shown in **Tables 7 and 8.** Second-order rate constant k_2 in g $mg^{-1}min^{-1}$ and adsorption capacity q_e in mg/g are obtained theoretically with the slope and intercept of the plots shown in **Fig 9 to 12** and the data analysis were shown in **Tables** 7 **and 8** respectively at the optimized conditions for both the metals.

Table 7: Pseudo second order equation at different adsorbent conditions for Cd (II)

PSOE Conditions	Model equation	k_2 (g mg^{-1} min^{-1})	q_e (mg/g)	R^2
pH 6	y = 0.1342x + 1.2341	0.0146	7.45	0.97
T = 40 °C	y = 0.1111 x + 0.6903	0.018	9	0.995
MIC of 100 ppm	y = 0.0606x + 0.2571	0.0143	16.5	0.999
Ads dosage = 5 g/L	y = 1.0808x + 1.7903	0.652	0.925	0.999

Table 8: Pseudo-second order equation at different adsorbent conditions for Cu (II)

PSOE Conditions	Model equation	k_2 (g mg^{-1} min^{-1})	q_e (mg/g)	R^2
pH 6	y = 0.103x + 0.218	0.0486	9.7	0.999
T = 40°C	y = 0.098x + 0.5086	0.019	10.2	0.998
MIC = 100 ppm	y = 0.055x + 0.0989	0.03	18.18	0.9993

Ads dosage = 5 g/L	y = 1.001x + 0.9317	1.075	0.999	0.9999

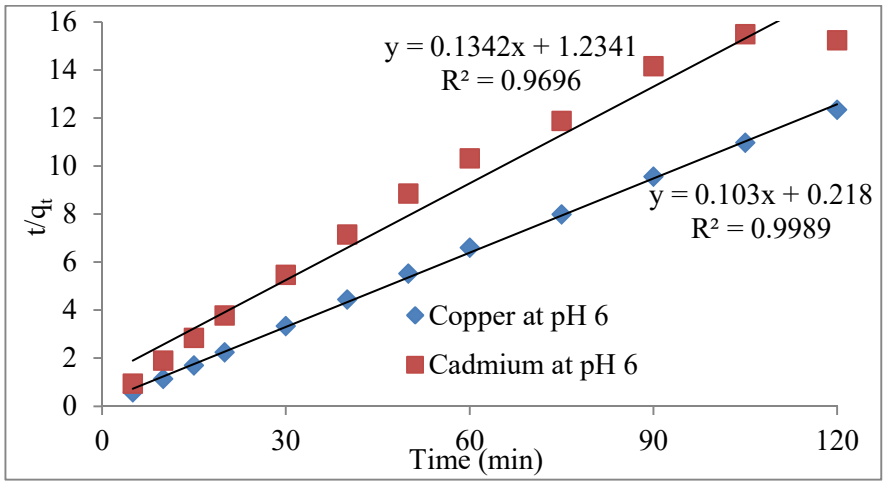

Fig 9: Pseudo second order equation for copper and cadmium at pH 6

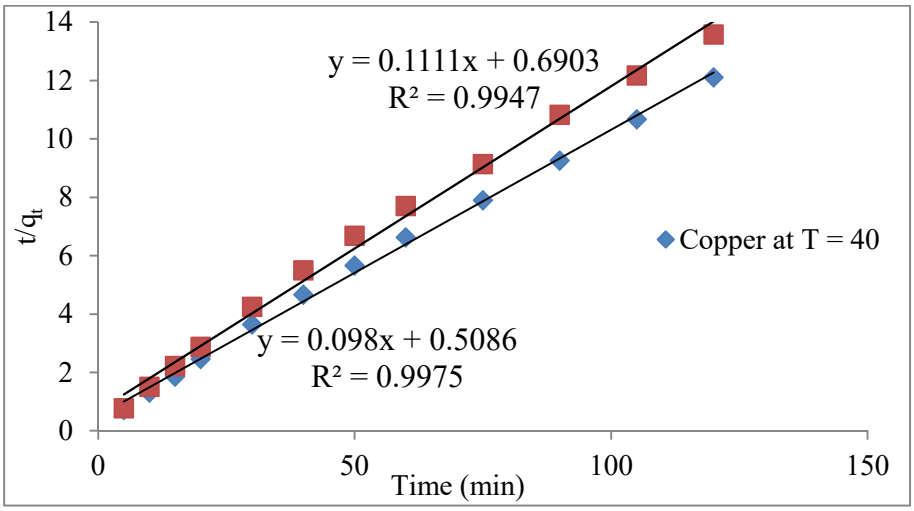

Fig 10 Pseudo second order equation for copper and cadmium at T = 40°C

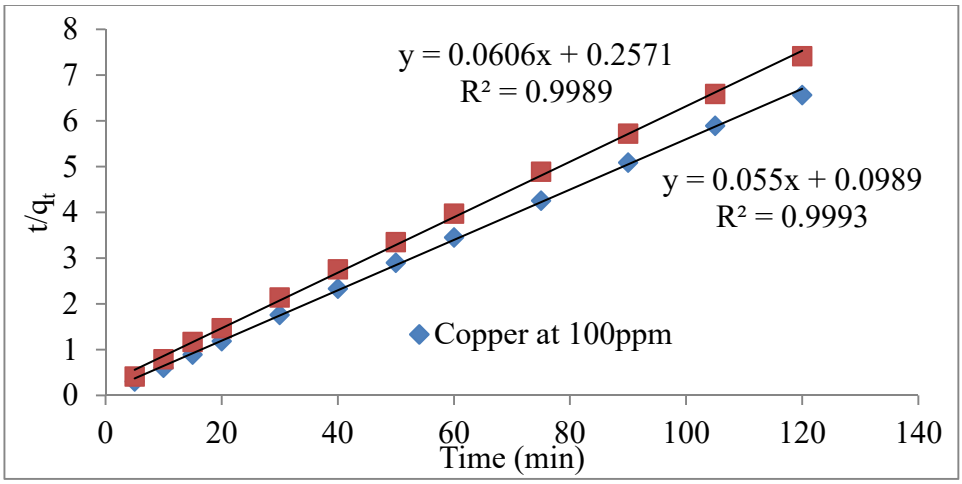

Fig 11 Pseudo second order equation for copper and cadmium at MIC of 100 ppm

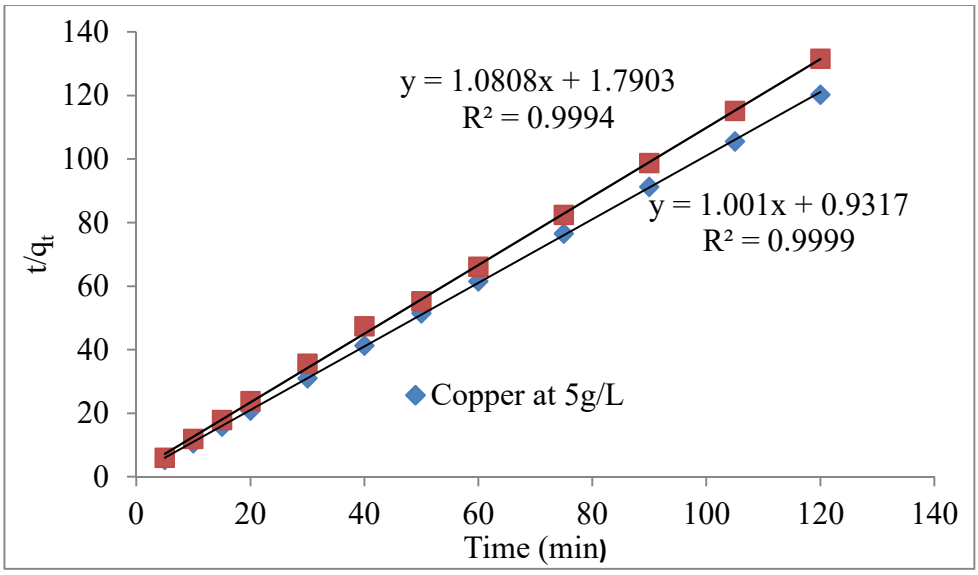

Fig 12 Pseudo-second order equation for copper and cadmium at 5 g/L of adsorbent dosage

3.2 Statistical analysis

The statistical analysis of copper and cadmium at different temperatures and various optimized parameters for synthetic solution data have been shown in **Tables 9 to 16** along with statistical parameter (χ^2) values. The statistical analysis has been carried out to find out the χ^2values using Langmuir model for copper and cadmium which indicates the least values of χ^2 values for better suitability of the model study and to find the reaction mechanism [29] The equilibrium adsorptive capacities (q_{eq}) theoretical values were obtained from the Langmuir plot at different temperatures given by **Eq.6** as shown below.

$$\frac{C_{eq}}{q_{eq}} = \frac{1}{bq_{max}} + \frac{1}{q_{max}} C_{eq} \qquad (6)$$

In comparison of statistical analysis for copper and cadmium from the above **Tables 9 and 10** the χ^2 values were less for copper when compared to cadmium at 25, 30, 35 and 40 °C which denotes the supremacy with lower or insignificant values and further suggest the dominance of χ^2 (statistical parameter) value for copper.

In the present investigation the reaction kinetic model aptness was also proficient by executing the statistical analysis, i.e, by calculating the χ^2 test (χ^2 value) via the experimental and theoretical data of uptake capacity (mg/g). The below **Eq.7** gives the assessment of fitting the data for reaction kinetic models.

$$\chi^2 = \frac{[(q_{exp} - q_{the})]^2}{q_{the}} \qquad (7)$$

The values of χ^2 with their respective models have been shown in **Tables 11 to 13** for copper and **Tables 14 to 16** for cadmium. The statistical analysis of the data attained in reaction kinetic modeling outlined the control of Pseudo-second order model for both Cu and Cd with very low or insignificant χ^2 values, when associated with the pseudo-first order model and Langmuir model with higher χ^2 values at different optimized conditions and thereby suggesting the dominance for both Cu (II) and Cd (II) ion adsorption mechanism as chemisorption instead of physical adsorption [30] [31]

Table 9 Statistical analysis of copper at different temperatures for synthetic solution

S.No	T (°C)	$q_{max}(q_{the})$	q_e (q_{exp})	(q_{exp}-q_{the})	(q_{exp}-q_{the})^2	$\chi^2 = \frac{[(q_{exp} - q_{the})]^2}{q_{the}}$
1	25	8.46	9.114	0.654	0.4277	0.0505
2	30	7.91	9.171	1.261	1.590	0.201
3	35	8.27	8.977	0.707	0.499	0.0604
4	40	7.24	8.707	1.467	2.152	0.2972

Table 10 Statistical analysis of cadmium at different temperatures for synthetic solution

S.No	T (°C)	$q_{max}(q_{the})$	q_e (q_{exp})	(q_{exp}-q_{the})	(q_{exp}-q_{the})^2	$\chi^2 = \frac{[(q_{exp} - q_{the})]^2}{q_{the}}$
1	25	4	5.92	1.92	3.6864	0.922
2	30	4.62	6.81	2.19	4.7961	1.038
3	35	5.11	6.95	1.84	3.3856	0.663
4	40	5.74	7.53	1.79	3.2041	0.558

Table 11 Statistical analysis for Langmuir equation at optimized parameters for copper

S.No	Optimized Parameter	$q_{max}(q_{the})$	q_e (q_{exp})	(q_{exp}-q_{the})	(q_{exp}-q_{the})^2	$\chi^2 = \frac{[(q_{exp} - q_{the})]^2}{q_{the}}$
1	pH 6	8.446	9.114	0.668	0.4462	0.053

2	T = 40	7.24	8.707	1.467	2.1521	0.297
3	MIC 100ppm	14.75	17.178	2.428	5.895	0.4
4	Ads dose 5g/l	0.942	0.969	0.027	0.00073	0.001

Table 12 Statistical analysis for Pseudo first order equation at optimized parameters for copper

S.No	Optimized Parameter	$q_{max}(q_{the})$	q_e (q_{exp})	$(q_{exp}-q_{the})$	$(q_{exp}-q_{the})^2$	$\chi^2 = \frac{[(q_{exp}-q_{the})]^2}{q_{the}}$
1	pH 6	1.198	9.114	7.916	62.663	52.306
2	T = 40	3.234	8.707	5.473	29.953	9.262
3	MIC 100ppm	0.646	17.178	16.532	273.31	423.076
4	Ads dose 5g/l	0.062	0.969	0.907	0.8226	13.269

Table 13 Statistical analysis for Pseudo second order equation at optimized parameters for copper

S.No	Optimized Parameter	$q_{max}(q_{the})$	q_e (q_{exp})	$(q_{exp}-q_{the})$	$(q_{exp}-q_{the})^2$	$\chi^2 = \frac{[(q_{exp}-q_{the})]^2}{q_{the}}$
1	pH 6	9.708	9.114	-0.594	0.353	0.036
2	T = 40	10.204	8.707	-1.497	2.241	0.22
3	MIC 100ppm	18.18	17.178	-1.002	1.004	0.055
4	Ads dose 5g/l	0.999	0.969	-0.03	0.0009	0.001

Table 14 Statistical analysis for Langmuir equation at optimized parameters for Cadmium

S.No	Optimized Parameter	$q_{max}(q_{the})$	q_e (q_{exp})	$(q_{exp}-q_{the})$	$(q_{exp}-q_{the})^2$	$\chi^2 = \frac{[(q_{exp}-q_{the})]^2}{q_{the}}$
1	pH 6	4.001	5.92	1.919	3.68	0.92
2	T = 40	5.74	7.53	1.79	3.204	0.558
3	MIC 100ppm	9.92	14.41	4.49	20.16	2.032
4	Ads dose 5g/l	0.766	0.876	0.11	0.0121	0.0158

Table 15 Statistical analysis for Pseudo first order equation at optimized parameters for cadmium

S.No	Optimized Parameter	$q_{max}(q_{the})$	q_e (q_{exp})	$(q_{exp}-q_{the})$	$(q_{exp}-q_{the})^2$	$\chi^2 = \frac{[(q_{exp}-q_{the})]^2}{q_{the}}$

1	pH 6	1.895	5.92	4.025	16.2	8.549
2	T = 40	3.78	7.53	3.75	14.06	3.72
3	MIC 100ppm	4.34	14.41	10.07	101.405	23.365
4	Ads dose 5g/l	1.62	0.876	-0.744	0.5535	0.3417

Table 16 Statistical analysis for Pseudo second order equation at optimized parameters for cadmium

S.No	Optimized Parameter	$q_{max}(q_{the})$	q_e (q_{exp})	$(q_{exp}-q_{the})$	$(q_{exp}-q_{the})^2$	$\chi^2 = \frac{[(q_{exp}-q_{the})]^2}{q_{the}}$
1	pH 6	7.451	5.92	-1.531	2.344	0.315
2	T = 40	9	7.53	-1.47	2.161	0.24
3	MIC 100ppm	16.5	14.41	-2.09	4.368	0.265
4	Ads dose 5g/l	0.925	0.876	-0.049	0.0024	0.0026

3.3 Isotherm modeling studies for simultaneous metal ion (Cu and Cd) removal in batch studies.

In this isothermal modeling Langmuir model, Temkin model have been studied for both the metals copper and cadmium.

3.3.1 Analysis of Langmuir Isotherm data for simultaneous Cu (II) & Cd (II) removal

It was concluded from the **Table 17** that the separation factor (R_L) values are (< 1) indicating that Langmuir model is an favorable adsorption isotherm model for individually Cu (II) and Cd (II) at 25°C, different adsorbent dosage, agitation rate of 180 rpm, pH 6 and contact time of 2hrs. Moreover, correlation coefficients (R^2) values are in the range of 0.8 to 0.98 which predicts the better suitability and fitting of the models for both Cu (II) and Cd (II). The higher R^2 values are seen in case of Cu (II) which predicts the better suitability when compared to Cd. The graphs for Langmuir isotherm model (c_e and c_e/q_e) at different adsorbent dosages of (5, 3, 2, 1, 0.5 g/L) and at various initial adsorbent conditions (pH 6, 180 rpm, 2 hrs contact time, temperature of 25°C) were shown in **Figs. 13 to 17** respectively for both the metals [32] [33]

Table 17 Analysis of Langmuir Isotherm data for simultaneous Cu (II) and Cd (II) removal

Metal	Ads dose (g/L)	Slope ($1/q_{max}$)	Intercept ($1/ bq_{max}$)	q_{max} (Max ads capacity, mg/g)	b (Langmuir Isotherm constant)	Initial concentration (C_o)	Separation factor R_L	R^2
Cd	5	4.3	-35.3	0.232	-0.12181	25.74	-0.2	0.97
Cu	5	2.32	-11.45	0.431	-0.20262	50	-0.13	0.98
Cd	3	4.25	-59.35	0.235	-0.07161	25.74	-0.39	0.95

Cu	3	3.26	-47.85	0.306	-0.06813	50	-0.52	0.98
Cd	2	7.04	-159	0.142	-0.04428	25.74	-0.82	0.94
Cu	2	4.02	-89.25	0.248	-0.04504	50	-1.07	0.96
Cd	1	7.21	-199.45	0.138	-0.03615	25.74	-1.24	0.95
Cu	1	2.99	-78.35	0.334	-0.03816	50	-1.56	0.888
Cd	0.5	31.21	-1097.9	0.032	-0.02843	25.74	-2.37	0.725
Cu	0.5	5.23	-178.1	0.1912	-0.02937	50	-3.81	0.798

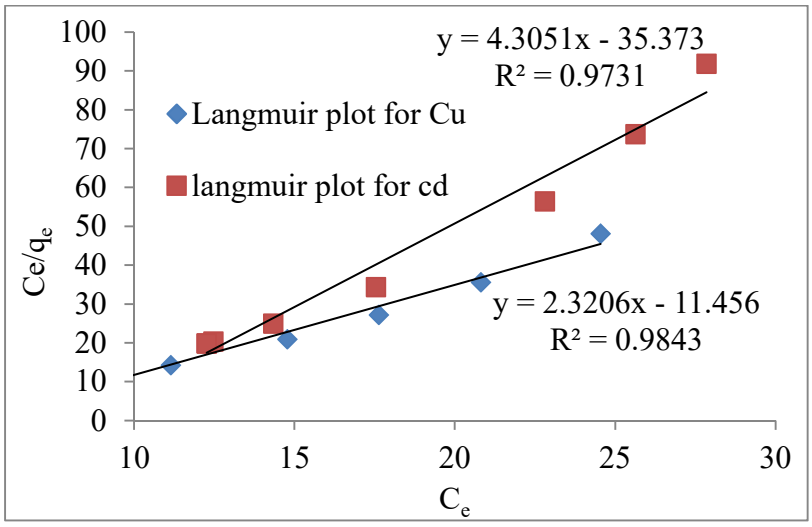

Fig 13 Langmuir isotherm model for Cu and Cd at 5g/L of ads dosage, pH 6, 180rpm, 2hrs contact time, 25ºC

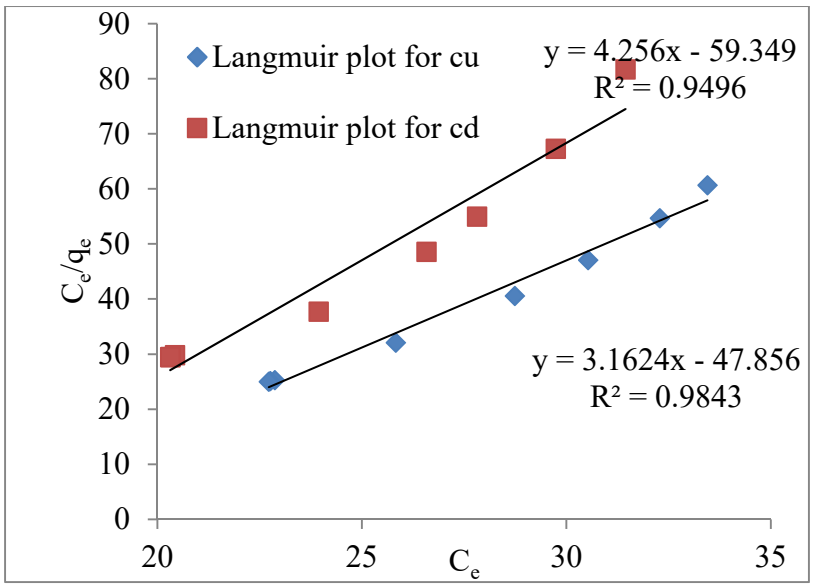

Fig 14 Langmuir isotherm model for Cu and Cd at 3g/L of ads dosage, pH 6, 180rpm, 2hrs contact time, 25ºC

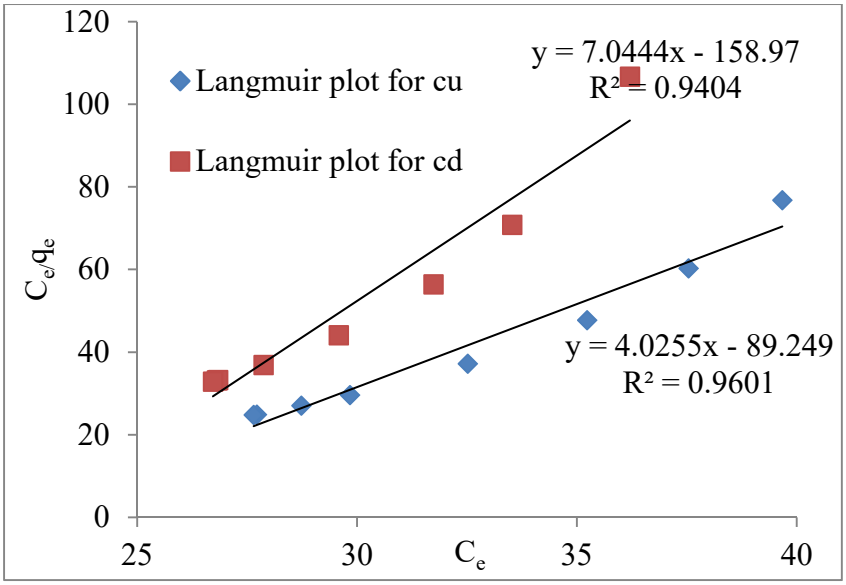

Fig 15 Langmuir isotherm model for Cu and Cd at 2g/L of ads dosage, pH 6, 180rpm, 2hrs contact time, 25°C

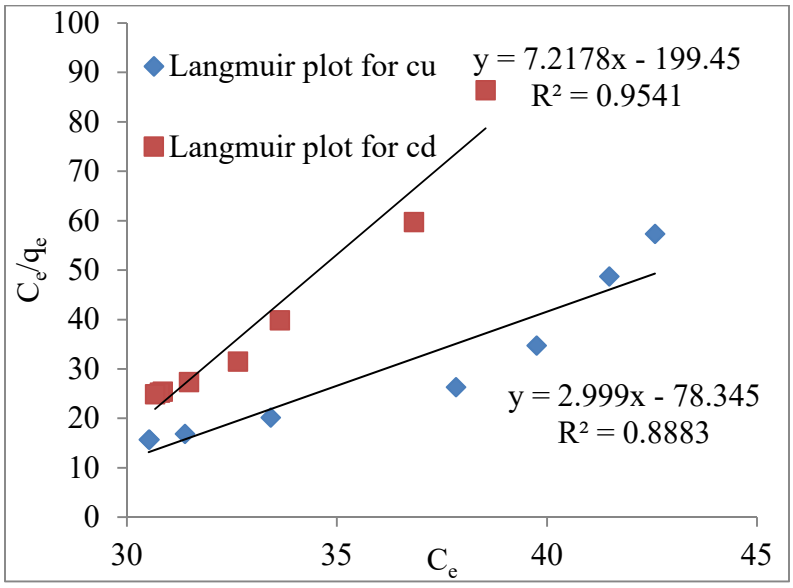

Fig 16 Langmuir isotherm model for Cu and Cd at 1g/L of ads dosage, pH 6, 180rpm, 2hrs contact time, 25°C

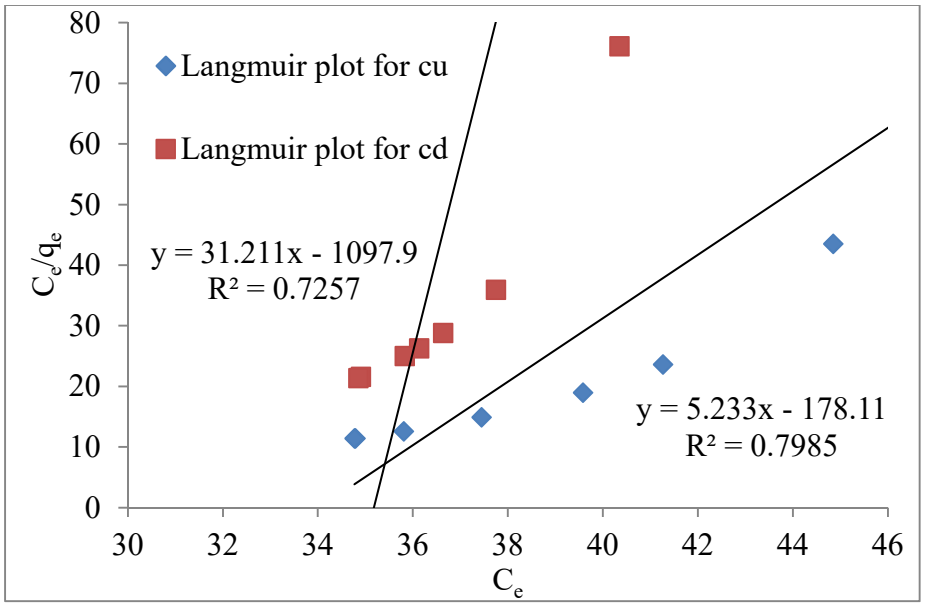

Fig 17 Langmuir isotherm model for Cu and Cd at 0.5 g/L of ads dosage, pH 6, 180rpm, 2 hrs contact time, 25°C

3.4 Temkin model

The Temkin isotherm model was given as follows described by **Eq 8 and 9**

$$q_e = B_t (\ln K) + B_T (\ln C_e) \quad (8)$$

$$\text{Where } B_T = \frac{RT}{b} \quad (9)$$

Where the constant B_T is interrelated with the heat of adsorption or the variation of adsorption energy in (J/mol). R = universal gas constant (J/ mol K), T = temperature (K). A plot of q_e versus ln C_e assists the determination of the isotherm constants B_T and K from the slope and the intercept, respectively [31–33]. **Fig 18** shows the Temkin isotherm model for Cu and Cd at 5g/l of ads dosage and different adsorbent conditions.

3.4.1 Analysis of Temkin model

Temkin model has been studied for the obtained data and the variation of heat of adsorption (B_T) for Cu and Cd has been found at 5g/l. More over higher R^2 values for both Cu (II) and Cd (II) predicts the suitability of this isotherm model at the given adsorbent conditions. The value of B_T (heat of adsorption) for Cu (II) and Cd (II) at 5g/l of adsorbent dosage are -0.31, -0.37 J/mol respectively. The Temkin isotherm constant values were reported as 0.0072 for Cu and 0.0151 for Cd respectively as shown in **Table 18** respectively. **Fig 18** shows the Temkin isotherm model for Cu and Cd at 5g/L of ads dosage and different adsorbent conditions of pH 6, 2 hrs contact time and temperature of 25°C. It was concluded that Langmuir model and Temkin models fit the simultaneous Cu and Cd removal in batch studies with higher R^2 values.

Table 18 Analysis of Temkin isotherm data for simultaneous cu (II) and cd (II) removal

Metal	Ads dose	Slope (B_T)	Intercept ($B_T \ln K_T$)	ln (K_T)	K_T	R^2
Cu	5g/l	-0.306	1.51	-4.934	0.007193	0.986
Cd	5g/l	-0.3696	1.5486	-4.19	0.015147	0.99

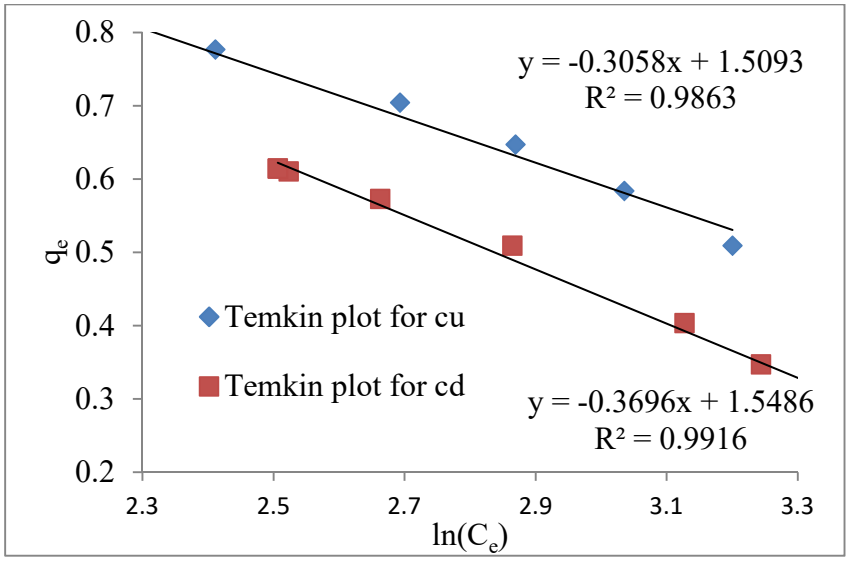

Fig 18 Temkin isotherm model for Cu and cd at 5 g/L of ads dosage, pH 6, 180rpm, 2hrs contact time, 25°C

Conclusions

It was concluded that the coefficient of regression R^2 values are almost 1 indicating that the adsorption system fits equally well with the Pseudo first order equation for both the metals Cu (II) and Cd (II). In case of second order system the coefficient of regression R^2 values are nearly 1 indicating that the adsorption system follows the second-order kinetics for both Cu (II) and Cd (II) metals. In comparison of both the models, the Pseudo-second order kinetics follows the best fit for both Cu (II) and Cd (II) with higher R^2 values very close to 1. It has been shown that mixed adsorbent appears to be technically feasible sorbent material with high efficiency and removing capability of metal ions. Consequently, the mixed adsorbent can be recommended to use for the removal of other heavy metal ions from complex industrial discharges.

The conclusions from the batch study give the highest % removal of metal ions with respect to time at optimized parameters for both the metals.

pH 6 Adsorbent dosage of 5g IMC of 50 ppm Temperature of 40°C Contact time of 120 min

Agitation rate of 180rpm

Pseudo First order equation (PFOE) fits for Cd (II) and Cd (II) with higher R^2 values close to 1. Pseudo Second order equation (PSOE) fits for Cu (II) and Cd (II) with higher R^2 values close to 1. In the simultaneous metal ion removal, it was concluded that Langmuir model and Temkin models fit the simultaneous Cu and Cd removal in batch studies

with higher R^2 values. The statistical analysis of the data attained in kinetic modeling outlined the control of Pseudo-second order model for both Cu and Cd with very low or insignificant χ^2 values, when compared with the pseudo-first order model and Langmuir model with higher χ^2 values at different optimized conditions and thereby suggesting the dominance for both Cu (II) and Cd (II) ion adsorption mechanism as chemisorption instead of physical adsorption.

The conclusion gave the overview on the mixed adsorbent prepared by mixing activated charcoal and bone charcoal in 1:1 ratio can be taken as a best adsorbent for heavy metal ion removal. These mixed adsorbent studies can be extended to various complex industrial effluents that contains the concentration range of 100-300 ppm and can be applicable to know the interaction between various parameters with respect to % removal in batch studies.

REFERENCES

1. Lasheen MR, Ammar NS, Ibrahim HS (2012) Adsorption/desorption of Cd(II), Cu(II) and Pb(II) using chemically modified orange peel: Equilibrium and kinetic studies. Solid State Sciences 14:202–210. https://doi.org/10.1016/j.solidstatesciences.2011.11.029
2. Iskandar NL, Zainudin NAIM, Tan SG (2011) Tolerance and biosorption of copper (Cu) and lead (Pb) by filamentous fungi isolated from a freshwater ecosystem. Journal of Environmental Sciences 23:824–830. https://doi.org/10.1016/S1001-0742(10)60475-5
3. Zhu CS, Wang LP, Chen W bin (2009) Removal of Cu(II) from aqueous solution by agricultural by-product: Peanut hull. Journal of Hazardous Materials 168:739–746. https://doi.org/10.1016/j.jhazmat.2009.02.085
4. Pohanish RP (2012) Sittig's Handbook of Toxic and Hazardous Chemicals and Carcinogens, 6th ed. Elsevier, Waltham
5. Ferrari L, Kaufmann J, Winnefeld F, Plank J (2010) Interaction of cement model systems with superplasticizers investigated by atomic force microscopy, zeta potential, and adsorption measurements. Journal of Colloid and Interface Science 347:15–24. https://doi.org/10.1016/j.jcis.2010.03.005
6. Babel S, Kurniawan TA (2003) Low-cost adsorbents for heavy metals uptake from contaminated water: A review. Journal of Hazardous Materials 97:219–243. https://doi.org/10.1016/S0304-3894(02)00263-7
7. Nwabanne JT, P.K.Igbokwe (2008) Kinetics and Equilibrium Modeling of Nickel Adsorption by Cassava Peel
8. Nishijima W, Akama T, Shoto E, Okada M (1997) Effects of adsorbed substances on bioactivity of attached bacteria on granular activated carbon. International Association on Water Quality
9. Jyoti (2013) Micropropagation of Hazelnut (Corylus Species). Thesis
10. Wang Y, Reardon EJ (2001) Activation and regeneration of a soil sorbent for defluoridation of drinking water. Applied Geochemistry 16:531–539. https://doi.org/10.1016/S0883-2927(00)00050-0
11. Lounici H, Addour L, Belhocine D, et al (1997) Study of a new technique for fluoride removal from water. Desalination 114:241–251. https://doi.org/10.1016/S0011-9164(98)00016-2
12. Srimurali M, Pragathi A, Karthikeyan J (1998) A study on removal of fluorides from drinking water by adsorption onto low-cost materials. Environmental Pollution 99:285–289. https://doi.org/10.1016/S0269-7491(97)00129-2

13. Durmaz F, Kara H, Cengeloglu Y, Ersoz M (2005) Fluoride removal by donnan dialysis with anion exchange membranes. Desalination 177:51–57. https://doi.org/10.1016/j.desal.2004.11.016
14. Choi WW, Chen KY (1979) Removal of Fluoride From Waters By Adsorption. Journal / American Water Works Association 71:562–570. https://doi.org/10.1002/j.1551-8833.1979.tb04420.x
15. Renge VC, Khedkar S V, Pande S V (2012) Removal of Heavy Metals From Wastewater Using Low Cost Adsorbents : a Review. Scientific Reviews and Chemical Communications Journal 2:580–584. https://doi.org/10.2147/SAR.S24800
16. Ma Y, Shi F, Wu M (2012) Removal of fluoride from aqueous solution by using Ca-bentonite and H-bentonite. Advanced Materials Research 391–392:1417–1422. https://doi.org/10.4028/www.scientific.net/AMR.391-392.1417
17. Kagne S, Jagtap S, Dhawade P, et al (2008) Hydrated cement: A promising adsorbent for the removal of fluoride from aqueous solution. Journal of Hazardous Materials 154:88–95. https://doi.org/10.1016/j.jhazmat.2007.09.111
18. Adsorbent N, Malay DK, Salim AJ (2018) Comparative Study of Batch Adsorption of Fluoride Using Commercial and Comparative Study of Batch Adsorption of Fluoride Using Commercial and Natural Adsorbent. 1:68–75
19. Veeraputhiran V, Alagumuthu G (2011) Treatment of High Fluoride Drinking Water Using Bioadsorbent. JChemSci_____Research Journal of Chemical Sciences 1:49–54
20. Valencia-Leal S a., Cortés-Martínez R, Alfaro-Cuevas-Villanueva R (2012) Evaluation of Guava Seeds (Psidium Guajava) As a Low- Cost Biosorbent for the Removal of Fluoride from Aqueous Solutions. International Journal of Engineering Research and Development 5:69–76
21. Oboh OI, Aluyor EO (2008) The removal of heavy metal ions from aqueous solutions using sour sop seeds as biosorbent. African Journal of Biotechnology 7:4508–4511. https://doi.org/10.4314/ajb.v7i24.59630
22. Faria PCC, Órfão JJM, Pereira MFR (2004) Adsorption of anionic and cationic dyes on activated carbons with different surface chemistries. Water Research 38:2043–2052. https://doi.org/10.1016/j.watres.2004.01.034
23. Celik A, Demirbaş A (2005) Removal of heavy metal ions from aqueous solutions via adsorption onto modified lignin from pulping wastes. Energy Sources 27:1167–1177. https://doi.org/10.1080/00908310490479583
24. Gong R, Ding Y, Liu H, et al (2005) Lead biosorption and desorption by intact and pretreated spirulina maxima biomass. Chemosphere 58:125–130. https://doi.org/10.1016/j.chemosphere.2004.08.055
25. Fenti A, Chianese S, Iovino P, et al (2020) Cr(VI) sorption from aqueous solution: A review. Applied Sciences (Switzerland) 10:. https://doi.org/10.3390/APP10186477
26. Ko DCK, Porter JF, McKay G (2000) Optimized correlations for the fixed-bed adsorption of metal ions on bone char. Chemical Engineering Science 55:5819–5829. https://doi.org/10.1016/S0009-2509(00)00416-4
27. Tomar V, Kumar D (2013) A critical study on efficiency of different materials for fluoride removal from aqueous media. Chemistry Central Journal 7:1. https://doi.org/10.1186/1752-153X-7-51
28. Singh D, Tiwari A, Gupta R (2012) Phytoremediation of lead from wastewater using

aquatic plants. Journal of Agricultural Technology 8:1–11
29. Aharoni C, Ungarish M (1976) Kinetics of activated chemisorption. J Chem Soc, Faraday Trans I72:400–408
30. Ho YS, Kim Y, Kim C, et al (2004) Comment on “arsenic removal using meseporous alumina prepared via a templating method” (multiple letters). Environmental Science and Technology 38:3214–3216. https://doi.org/10.1021/es049688w
31. Nhapi I (2011) Removal of Heavy Metals from Industrial Wastewater Using Rice Husks. The Open Environmental Engineering Journal 4:170–180. https://doi.org/10.2174/1874829501104010170
32. Hasan SH, Singh KK, Prakash O, et al (2008) Removal of Cr(VI) from aqueous solutions using agricultural waste “maize bran.” Journal of Hazardous Materials 152:356–365. https://doi.org/10.1016/j.jhazmat.2007.07.006
33. Fiset JF, Blais JF, Riveros PA (2008) Review on the removal of metal ions from effluents using seaweeds, alginate derivatives and other sorbents. Revue des Sciences de l’Eau 21:283–308. https://doi.org/10.7202/018776ar